NDT&E International 59 (2013) 48–56

Contents lists available at SciVerse ScienceDirect

NDT&E International

journal homepage: www.elsevier.com/locate/ndteint

Transient thermography testing of unpainted thermal barrier coating (TBC) systems

Grzegorz Ptaszek [a], Peter Cawley [a,*], Darryl Almond [b], Simon Pickering [b]

[a] UK Research Centre in NDE, Imperial College London, UK
[b] UK Research Centre in NDE, University of Bath, UK

ARTICLE INFO

Article history:
Received 12 January 2013
Received in revised form
30 April 2013
Accepted 3 May 2013
Available online 16 May 2013

Keywords:
Transient thermography
Thermal barrier coating
TBC
Infrared wavelength
Signal processing
Thermal response
Disbond
Flat bottomed hole

ABSTRACT

Test piece surfaces are sometimes coated with a black, energy absorbing paint before transient thermography is applied. This practice is not acceptable to some thermal barrier coating (TBC) manufacturers and servicers of these systems since thermal barrier coatings are porous so the paint contaminates the coating and it is very difficult and costly to remove. Unfortunately, unpainted TBC surfaces have low emissivity, and after service their colour is usually uneven. The low emissivity gives low signal levels and also problems with reflections of the incident heat pulse, while the variation in emissivity over the surface gives strong variation in the contrast obtained even in the absence of defects. Additionally, the TBC is translucent to mid-wavelength IR radiation which negatively affects the location of disbonds based on the thermal responses. This paper investigates the effects of uneven discolouration of the surface and of IR translucency on the thermal responses. It has been shown that unpainted TBC systems can be inspected reliably by using higher power flash heating equipment assembled with an IR glass filter and a long wavelength IR camera. The paper also shows that the problem with uneven surface emissivity can be overcome by applying 2nd time derivative processing of the log–log surface cooling curves.

1. Introduction

Test piece surfaces are often painted black for thermography inspection in order to provide a uniform emissivity of around unity. However, covering a thermal barrier coating (TBC) system [1] with any form of paint is often not acceptable because of possible contamination of the porous ceramic coating by the paint. Painting of TBC surfaces and the difficult process of paint removal can be highly time consuming and also unacceptably expensive.

If during a standard transient thermography inspection a TBC specimen was covered by a highly absorbing paint layer, the photo-thermal effect would occur uniformly on the surface of the specimen and after that the specimen would cool down due to conduction of heat into the bulk of the specimen. At the same time, the specimen would emit thermal radiation from its surface as can be seen in Fig. 1a. Unfortunately, unpainted TBC causes difficulties during transient thermography tests, particularly when the coating has not been long in service. This is caused by part translucency to visible, near and middle IR radiation; therefore, the incident pulse of visible and IR light penetrates the coating (Fig. 1b) and the photo-thermal effect happens through the volume of TBC. The degree of translucency depends on the coating composition and its thickness [2,3].

Additionally, after the pulse of applied energy is switched off, the excitation source continues to emit thermal radiation (afterglow effect) which is reflected from the TBC and interferes with the emitted thermal radiation from the TBC (Fig. 1b). This interference negatively affects interpretation of the thermal images recorded by an IR camera. Furthermore, in most thermography applications, the wavelength of the IR camera which is used to monitor surface temperature is not an important consideration, since sample surfaces are generally IR opaque and emissive. However, TBC is not typical because when viewed in the mid-IR (2–5 μm) range it behaves differently to when viewed with long wave IR camera (8–14 μm). During testing of unpainted TBC, the mid wave IR camera receives emissions from the interior of the coating as well as the surface whereas the long wave IR registers emission only from the surface [4]. During service the translucency of TBC significantly decreases, but an additional problem arises as the surface colour tends to change non-uniformly, causing extensive variation of emissivity. For example, the passive, concave parts of the blades are mostly able to keep their original uniform bright yellow colour; however, the active convex parts become darker, even becoming black in some areas (Fig. 2).

In order to understand the mechanisms which affect the thermal responses when transient thermography is used for this specific application, firstly, the paper focuses on the influence of

* Corresponding author. Tel.: +44 2075947000.
E-mail address: p.cawley@imperial.ac.uk (P. Cawley).

0963-8695
http://dx.doi.org/10.1016/j.ndteint.2013.05.001

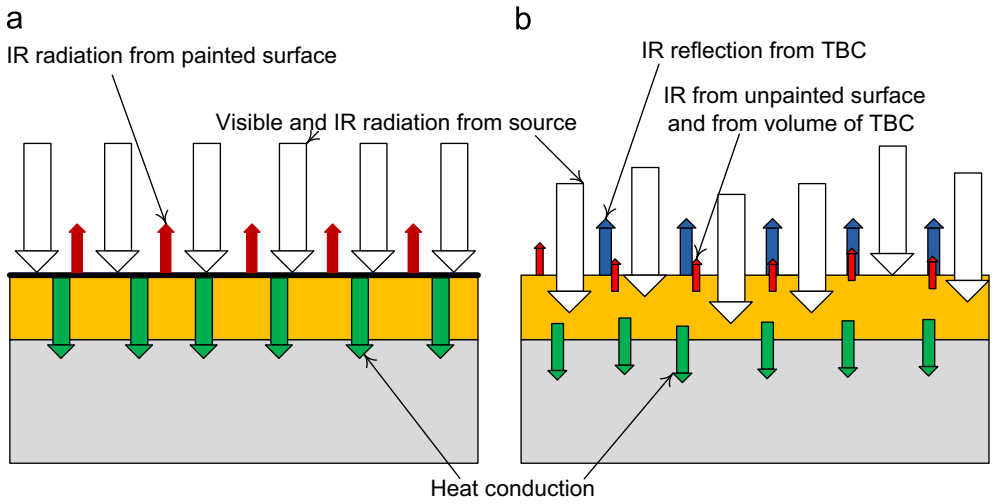

Fig. 1. Transient thermography effects during a test of TBC system: (a) painted; and (b) unpainted.

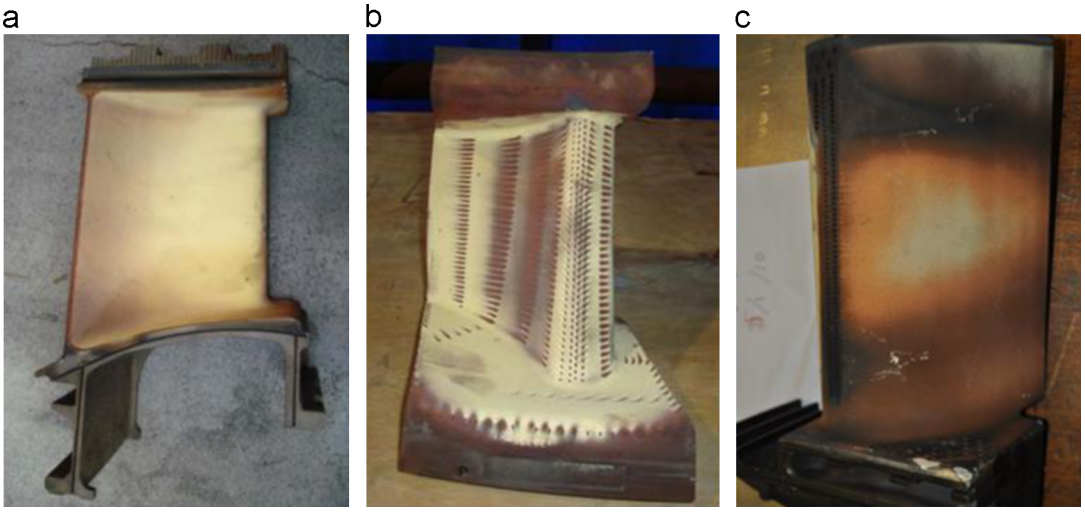

Fig. 2. Examples of unpainted TBC with surface discoloration on various types of TBC gas turbine blades (a) and (b) concave side; and (c) convex side. (For interpretation of the references to colour in this figure, the reader is referred to the web version of this article.)

TBC translucency to IR radiation and secondly, the effects of uneven energy absorption and emission caused by discolouration of the coating in service are discussed in detail. Section 2 describes a set of numerical simulations, while Section 3 reports transient thermography test results obtained with an appropriate transient thermography system applied on various test specimens. Section 4 proposes practical solutions to facilitate transient thermography of unpainted TBC systems.

2. Numerical simulations

2.1. Settings

In order to predict TBC surface temperature following pulse heat deposition in transient thermography, a finite element method was selected for the numerical solution of the problem. A set of TBC models was created in COMSOL [5], which was used to simulate conductive heat flow. The thermal and physical properties of all the material layers (nickel super alloy, zirconia, and air) were assumed to be homogenous and isotropic with the thermal properties given in Table 1.

Table 1
Thermo-physical properties used for simulations [6,7].

Layer (material)	Density ρ [kg/m^3]	Specific heat c [J/Kg K]	Conductivity k [W/mK]	Diffusivity α [m^2/s] $\times 10^{-6}$
Ceramic coat (90% zirconia, 10% air)	4680	460	1.35	0.63
Substrate and BC (nickel super alloy)	8400	455	14.8	3.87
Zirconia[a]	5200	400	2	0.96
Defect (air)	1.16	1007	0.026	22.2

[a] Properties applied for analytical solution presented in Fig. 11.

The modelled defects were located parallel to the surface, on the boundary between the zirconia coat and the nickel super alloy substrate, as they commonly occur in TBC systems. For each of the simulations, a model has been created to simulate a short heating pulse applied which can be seen in Ref. [1]. The role of the heating pulse was to stimulate the models in the same way as the pulse of energy stimulates TBC systems during the transient thermography test.

2.2. Coating translucency

As was indicated in the introduction, a new TBC coating absorbs optical energy not only on its surface, but also in its volume. In order to investigate the volumetric energy absorption and its effect on the TBC surface cooling, numerical simulations have been performed in which it was assumed that the energy was absorbed non-uniformly through the TBC layer; Bouguer's law has been applied for this purpose [8].

A 1D Comsol model has been created in which a pulse of energy with amplitude exponentially decreasing with depth from the surface was deposited at the same time on the layers of TBC in order to simulate simultaneous surface and volumetric energy absorption (translucency of TBC). The flux power density W per unit area was assumed to be given by

$$W = W_0 e^{-\gamma z} \tag{1}$$

where W_0 (2 kW/m^2 approximation of a real case) is the flux power density of incident radiation, γ is the medium absorption coefficient (2500 1/m) [9] and z is depth from the surface. For the model, the full thickness (l) of TBC was set to 0.8 mm so the flux power density at the bottom of the TBC was 13.5% of the value at the surface; the substrate was 4 mm thick.

Fig. 3 shows a comparison of the surface cooling on a log–log scale for this model, for semi-infinite TBC, and for black painted finite TBC rigidly attached to the substrate. The total amount of energy deposited is the same for all cases. The benefits of the log–log scale from which the first and the second time derivatives are calculated for a signal processing technique are described in Refs. [1,10–12].

As can be seen in Fig. 3, the maximum surface temperature was achieved when all the energy was deposited on the painted surface of TBC. The surface cooling for the translucent coating is slower in comparison to the surface cooling of black painted TBC due to the reduction of thermal gradient inside the TBC. In this situation, the energy was deposited in the volume and it was exponentially decaying from the surface through the thickness of the TBC. It is also possible to observe the accelerated surface cooling caused by the conductive substrate once the heat front reaches the TBC–metal boundary ($\sim$0.4 s).

The volumetric energy absorption has a negative effect on disbond detection when simple contrast images are used. In this scenario, slower surface cooling of a sound region will cause a reduction of the lateral thermal gradient on the surface between a defective region and a surrounding sound region and therefore the thermal contrast will reduce.

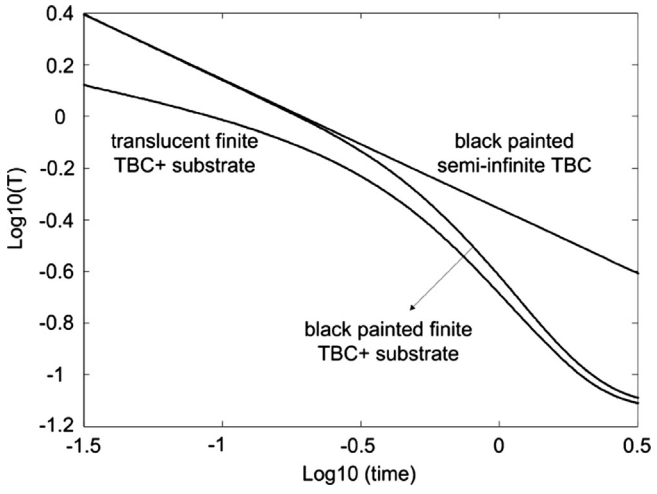

Fig. 3. Surface cooling as function of time on log–log scale for black painted semi-infinite TBC, finite black painted TBC bonded to substrate and finite translucent TBC bonded to substrate.

2.3. Effect of non uniform energy absorption on surface of TBC

Local changes of colour on TBC blades cause uneven absorption of optical energy and thermal emission of energy from the surface. Darker, and particularly black, regions will absorb and emit more energy than lighter regions of the TBC surface. Additionally, lighter regions might cause reflection of the radiation from the IR source.

In the models of Fig. 4 in which TBC is rigidly bonded (defects free) to the nickel super alloy substrate, only a region of TBC of radius varying from 0.6–4 mm received the pulse of energy. This configuration simulates the situation in which only the emissivity of a small selected region is equal to unity whereas the rest of the surface does not absorb energy. This region is marked in thick black showing that all energy only in this region has been absorbed. As can be clearly seen in Fig. 5 which shows the TBC surface cooling on a log–log scale, the size reduction of the region of unit emissivity causes some deviation of the cooling curves from their typical shapes (−0.5 slope).

However, this deviation becomes significant only when the spot diameter is less than around 1 mm. When the diameter is so small, lateral heat flow from the spot starts to dominate the surface cooling and as a result, the cooling is accelerated from the beginning. For regions with diameter greater than 1 mm, the surface cooling curves on a log–log scale have very similar shapes (Fig. 5) and the result of 2nd derivative processing will not be affected by the diameter. This is a benefit of the derivative approach because, as shown in the next section, regions which absorb more energy than the surroundings will produce thermal contrast which is liable to cause false calls if defect detection is based simple on contrast images.

In order to simulate how different levels of absorptivity/emissivity can affect the thermal responses from a defect, another set of models has been created where different heat fluxes were

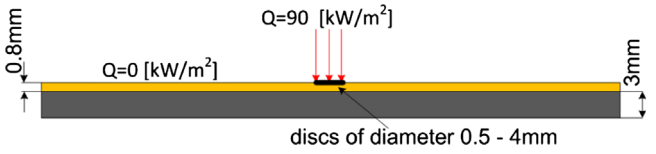

Fig. 4. Model of TBC plate rigidly connected to nickel-super alloy substrate. Pulse of energy applied only locally on circular regions of diameter 0.6–4 mm.

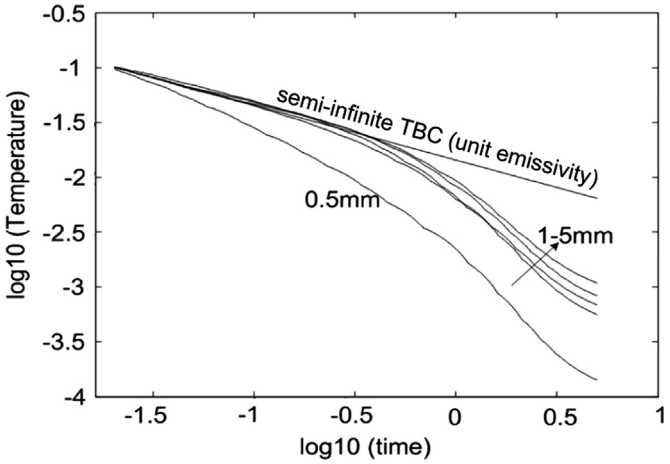

Fig. 5. Surface cooling on log–log scale for the model of Fig. 4.

applied to different regions of TBC rigidly bonded to the substrate for a duration of 50 ms (models: A–C Fig. 6). An artificial disbond [1] of diameter 4 mm (Model A) and 2 mm (Model B, C) having air gap thickness of 0.1 mm was placed between the TBC and the substrate. In model A, two local regions had greater heat flux applied than the rest of model. One of those regions of diameter 8 mm was placed above the defect and the second region of the same diameter was placed in a sound region. Also, in model B two local regions had greater heat flux applied than the rest of model. One of those regions of diameter 2 mm was placed above the defect and the second region of the same diameter was placed in a sound region. In model C, one region had reduced heat flux applied in comparison to the rest of the surface. This region had the same diameter as the defect and was placed above the defect. In model B the heat flux above the defect was increased in comparison to model A and the region of higher energy absorption was decreased to the diameter of the defect (2 mm). Additionally, the region of high energy deposition above the defect in all models has been displaced in steps of 2 mm from the centre of the defect in order to simulate how the position of a region of high emissivity might affect the thermal responses from a defect (Fig. 6). The change in heat flux above the defect between models A and B was chosen in order to simulate different emissivity/absorbivity levels. This increase in heat flux above the defect in model B in comparison to model A, together with the reduction in the diameter and the restriction of the region of high absorption to the diameter of the defect, represents an extreme case to investigate how lateral heat flow from the surface above the defect can affect the surface cooling curve.

As can be clearly seen in Fig. 7 generated from the models seen in Fig. 6, the maximum thermal contrast appears when the region of high emissivity is placed directly above the defect and

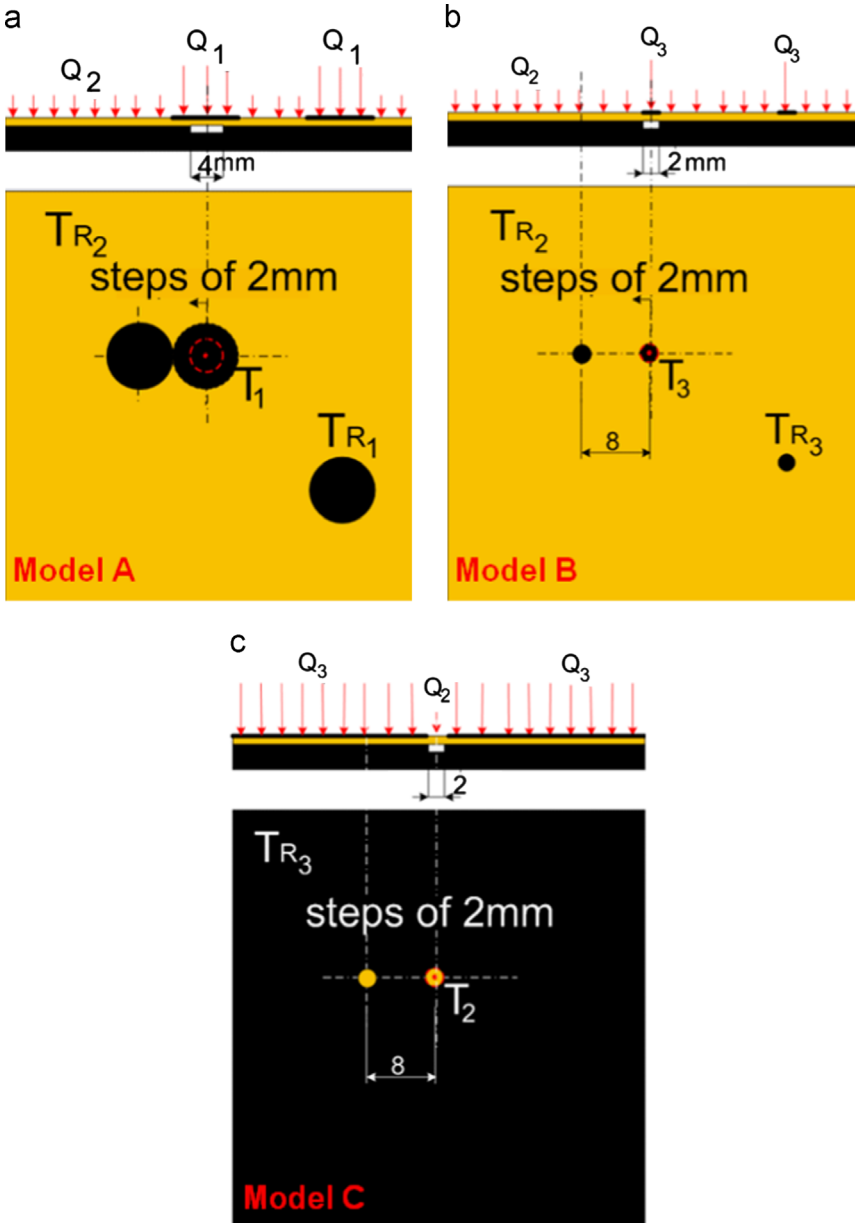

Fig. 6. Set of models with various amount of energy applied on TBC surface: Q_1, Q_3 represent areas of high emissivity (black) and Q_2 represents area of low emissivity; R_1, R_2, R_3 represent reference areas on which Q_1, Q_2, Q_3 is applied respectively. In each scenario, heat fluxes located above disbond have been displaced in steps of 2 mm (a) heat flux $Q_1=90$ kW/m^2, $Q_2=60$ kW/m^2; (b) heat flux $Q_3=120$ kW/m^2, $Q_2=60$ kW/m^2; and (c) heat flux $Q_2=60$ kW/m^2, $Q_3=120$ kW/m^2.

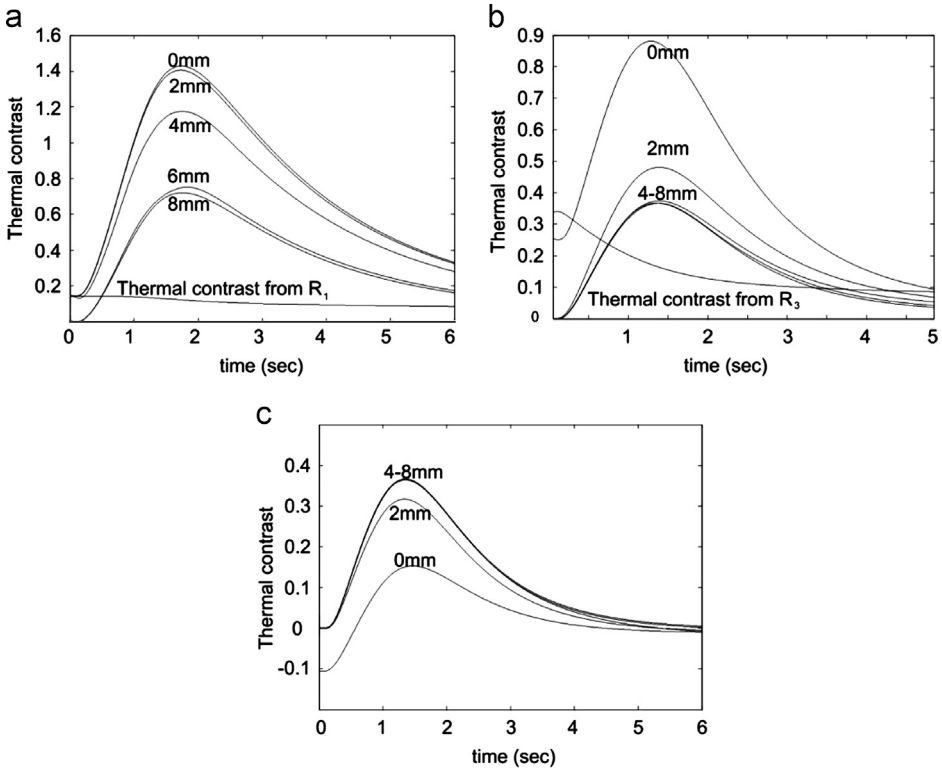

Fig. 7. Thermal contrast for models of Fig. 6 as function heat flux, time and distance between centre of defect and region of high emissivity. Additional thermal contrast generated on sound region caused by non-uniform emissivity: (a) heat flux $Q_1=90$ kW/m^2, $Q_2=60$ kW/m^2; (b) heat flux $Q_3=120$ kW/m^2, $Q_2=60$ kW/m^2; and (c) heat flux $Q_2=60$ kW/m^2, $Q_3=120$ kW/m^2.

increasing offset of this region causes a reduction of the thermal contrast. Fig. 7 shows also that there is a significant difference between the maximum thermal contrast in the model A (Fig. 7a) and B (Fig. 7b). There are two reasons for this: firstly the area of the defect in model A (Fig. 6a) is 4 times greater than in model B (Fig. 6b). Therefore, the lateral heat flow around the defect of smaller size causes reduction of the maximum thermal contrast and also the time when it appears [1]. Secondly, the amount of energy above the defect applied in the model A (Fig. 6a) is 12 times greater than in the model B (Fig. 6b) which results in the highest thermal contrast. In model C (Fig. 6c) the amount of energy directly above the defect is the smallest; therefore, the maximum thermal contrast has the lowest value. As the low emissivity region is moved away from the centre of the defect, the maximum thermal contrast increases, as would be expected. Additionally, in Fig. 7a and b thermal contrast is generated between regions of different emissivity even in the absence of a defect. This is undesirable since, even though an experienced operator would recognise that since the contrast is generated from the beginning it must be due to a surface feature, there is a danger that the presence of the signal will lead to mis-classification by some operators. Fig. 7 also shows that the time of the maximum thermal contrast is not affected by the position of the region of high emissivity.

The 2nd derivative calculated from log–log surface cooling shown in Fig. 8 allows clear distinction between defective and non defective regions. Additionally, the position, the size and the amount of energy deposited on regions of high absorptivity/emissivity (Model A, B Fig. 6a, b) only minimally affects the maximum value and the shape of the curves. The same situation is present for the model C (Fig. 6c). Therefore, these results suggest that application of the 2nd derivative processing for specimens that absorb energy non-uniformly is likely to give more reliable results than simple contrast processing.

3. Experimental results

As was indicated in the introduction, the transient thermographic inspection of unpainted TBC systems is made more difficult due to part translucency of TBC to visible, near and middle infrared, the afterglow effect and uneven absorptivity/emissivity of the coating. The problem of translucency can be successfully overcome by using a long wave length IR camera [2]. The afterglow effect can be significantly reduced by using a glass filter [13,14] and the problem with uneven absorptivity/emissivity of the coating might be eliminated by using the 2nd time derivative calculated from log–log surface cooling, as discussed above.

Therefore, a transient thermography system was employed comprising a PC for data analysis of the raw thermal images, a long wavelength (10 μm) IR camera and two flash lamps (6 kJ each) located in a container with a glass front. The container protected the lamps from damage and the glass filters out IR radiation from the source; this removed the afterglow effect [13,14]. An external system of cooling air was provided which cools both the lamps and the filter. The system and the principles of the approach can be seen in Fig. 9.

Knowing that in service TBC can change colour from its original white/yellow to black (Fig. 10a), three discs made of Zirconia (the main component of TBC) were prepared on which the effect on the surface cooling caused by five colours was investigated. The chosen colours possibly present in TBC in service were: white, yellow, orange, brown, and black (Fig. 10b). The diameter of each disc was 50 mm and their thickness was 3 mm. The colour was achieved by applying very thin layers of pastels. The thickness of the discs was 3 mm because thinner Zirconia is very fragile; TBC applied on a substrate can be much thinner and remain robust because it is supported. By using pastels, it was possible to apply a chosen colour homogeneously on an area of a satisfactory size to analyse the effect of the colour.

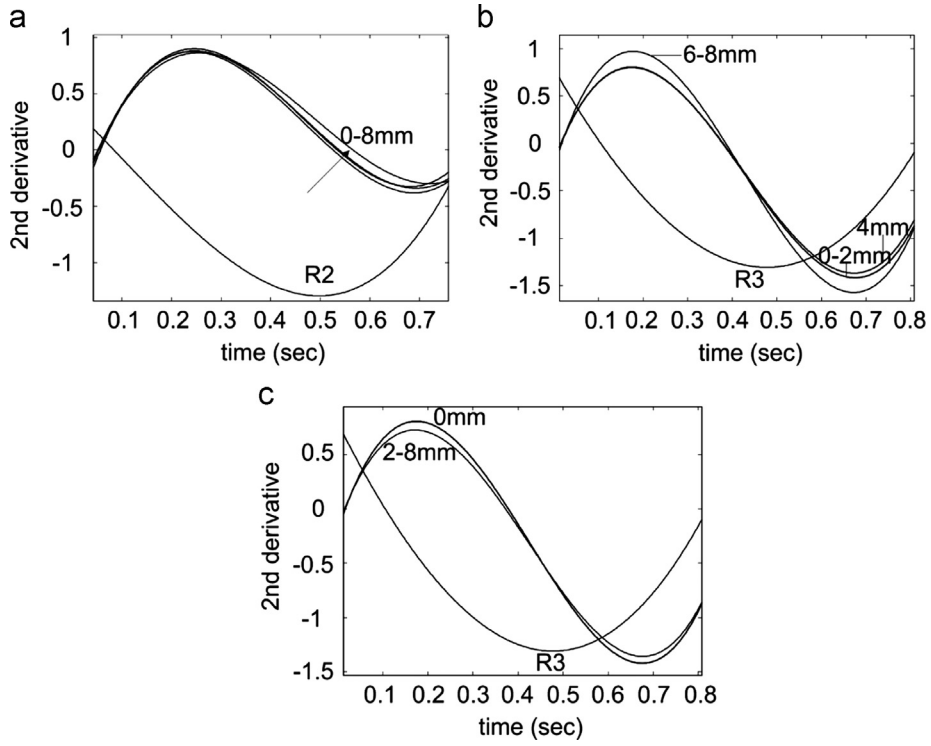

Fig. 8. 2nd Derivative from log (T)–log (t) surface cooling for models of Fig. 8 as function of heat flux, time and distance between centre of defect and centre of region of high emissivity: (a) heat flux $Q_1=90$ kW/m^2, $Q_2=60$ kW/m^2; (b) heat flux $Q_3=120$ kW/m^2, $Q_2=60$ kW/m^2; and (c) heat flux $Q_2=60$ kW/m^2, $Q_3=120$ kW/m^2.

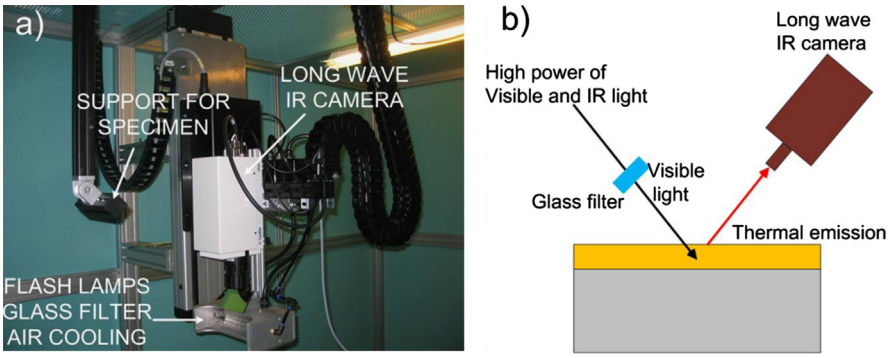

Fig. 9. (a) Transient thermography equipment applied; and (b) principles of tests.

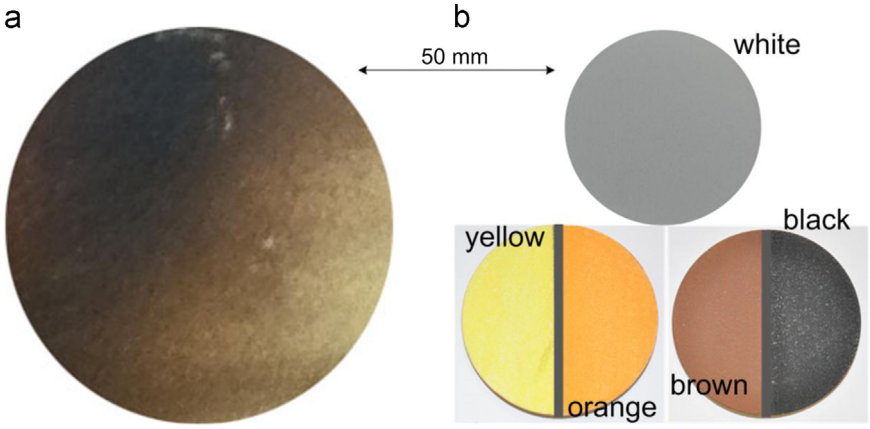

Fig. 10. (a) Selected region of zirconia TBC from blade in service; and (b) coloured zirconia discs. (For interpretation of the references to colour in this figure, the reader is referred to the web version of this article.)

In a real TBC environment, the colour change does not appear uniformly (Fig. 10a), and it is caused not only by impurities from the hot combustion gases attaching to the TBC surface, but also by decomposition of the top coating components at very high temperature [15]. Therefore, this complex process makes controlling the discolouration almost impossible.

Transient thermography tests were performed on the discs of Fig. 10b and thermal emission measurements were collected from five points in each area of interest and the averages were calculated. Fig. 11 presents the surface cooling collected from the discs plotted on a log–log scale together with the analytical solution for a 3 mm thick Zirconia plate. Firstly, the characteristic −0.5 cooling slope [1] already presented in Section 2.3 can be clearly seen. Secondly, the curves show the importance of the colour in visible light energy absorption and its emission where very clearly dark areas (brown and black) absorb and emit much more than the light coloured areas (white, yellow and orange). As was indicated already in Section 2.3, this uneven energy absorption and emission has a very strong influence on the thermal responses from a TBC specimen containing a defect which will be discussed in detail later.

The curve for the analytical solution (Fig. 11) was arbitrarily located between the white and yellow curves because the mixture of these colours most accurately represents the colour of a new ceramic coat. However, the surface temperature is a function of the amount of energy deposited in the flash as well as the surface colour, its roughness, the distance between the specimen and the energy source and also how the source and the specimen are positioned in relation to each other [16]. Therefore only the form of the theoretical curve should be compared with the measurements—the absolute temperature is a function of the other parameters that were not controlled in the experiments.

Fig. 12 shows the 2nd derivative calculated from the log–log surface cooling of Fig. 11. As can be clearly seen in Fig. 11, the maxima discussed in Ref. [1] are reached and they appear at about the time when the heat front reaches the bottom boundary of the discs. The time of the 2nd derivative maximum (t_d) can be used to measure the thickness of a layer when transient thermography is applied [13,17]. However, as can be seen in Fig. 12 there are some small but noticeable differences in the time of the 2nd derivative maximum between different colours (max around 0.4 s between black and white). These differences are likely to be caused by the uneven thickness of the applied pastel layers which were thin and therefore difficult to control.

A TBC reference specimen has been manufactured from a 6 mm thick nickel super alloy plate on which 1 mm thick TBC was applied. Seven FBHs of diameter 4 mm were introduced by using the technique described in Ref. [1]. The coating of the specimen was blackened at certain locations (Fig. 13) using small ink spots of diameter 4 and 2 mm placed above the FBHs. Black spots were also applied on sound regions; one spot of diameter 2 mm was made of a graphite layer (G); the rest of diameter 2 and 4 mm were made of paint layers (P).

Fig. 14a shows a photo of the specimen with all investigated areas (I–XI); this shows that the coating was damaged in two places during the manufacturing of the FBHs due to a human error which resulted in breakthrough of the holes. Fig. 14b shows the thermal image of the reference specimen in which as expected the blackened sound regions incorrectly indicate presence of the defects (areas IV, IX, X). As in the previous experiments, the surface cooling from the selected areas was plotted on a log–log scale (Fig. 15a). It can be clearly seen that the defective and the sound regions cool with the same −0.5 slope when the heat propagates inside of the coating after which, for the defective regions the surface cooling decelerates, whereas for the sound region it accelerates [1].

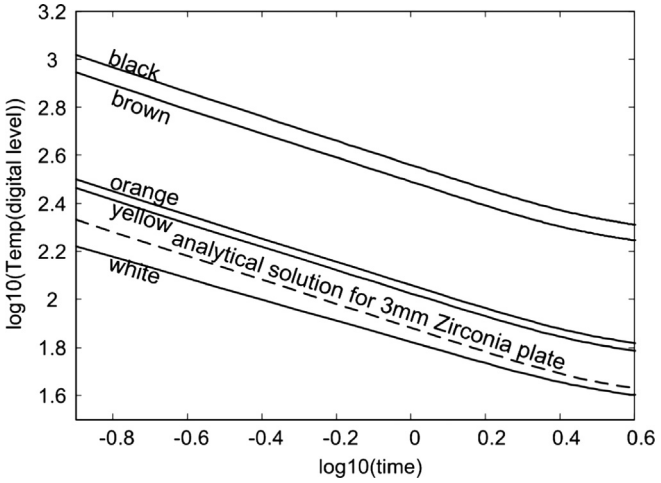

Fig. 11. Surface cooling on log–log scale from 3 mm thick discs of Fig. 12.

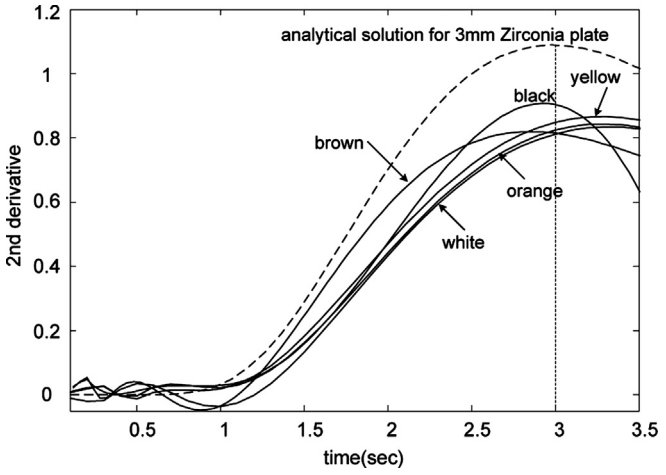

Fig. 12. 2nd Derivative calculated from log–log surface cooling of Fig. 13. Predicted curve for 3 mm zirconia plate TBC shown for comparison.

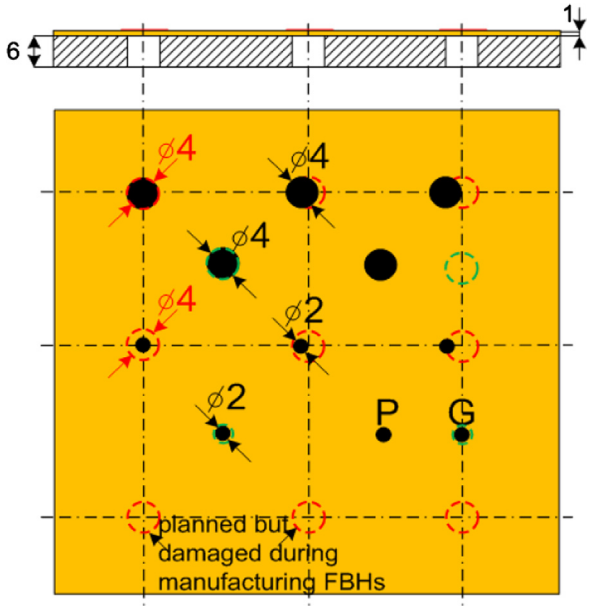

Fig. 13. TBC reference specimen with FBHs. Surface of TBC was locally blackened. Areas of interest are circled. On surface written two letters: P—paint, G—graphite.

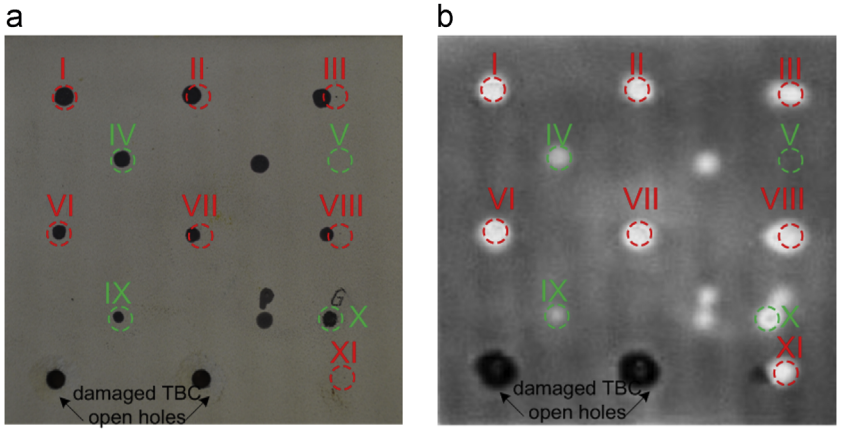

Fig. 14. TBC reference specimen of Fig. 13 (a) photo showing TBC specimen with areas of interest; and (b) thermal image of TBC specimen. (I, II, III, VI, VII, VIII, XI—defective regions; IV, V, IX, X—sound regions).

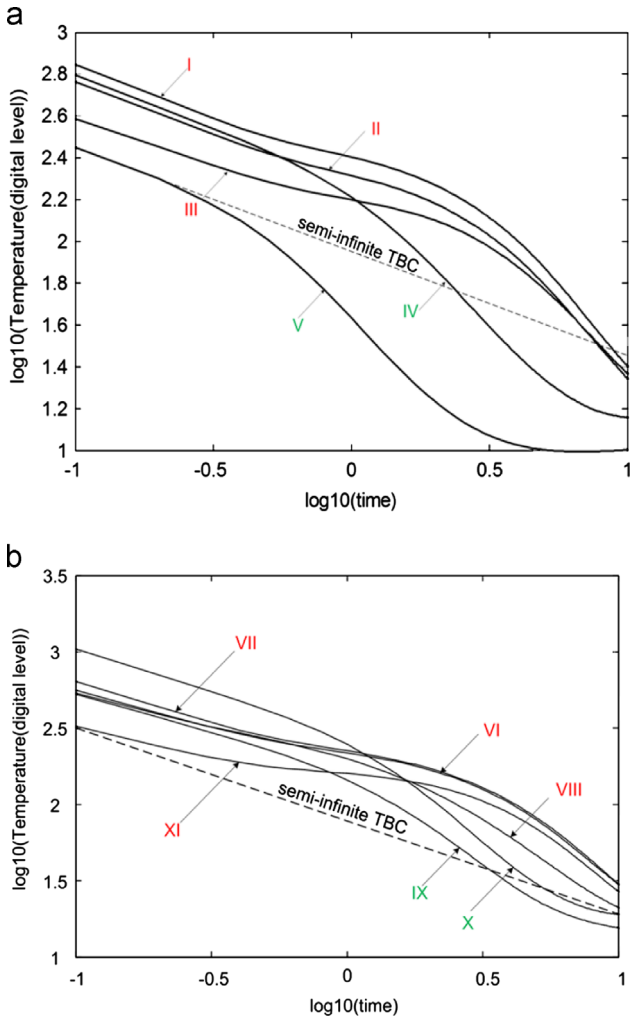

Fig. 15. (a) Surface cooling on log–log scale from areas I–V of Fig. 14; and (b) surface cooling on log–log scale from areas VI–XI of Fig. 14.

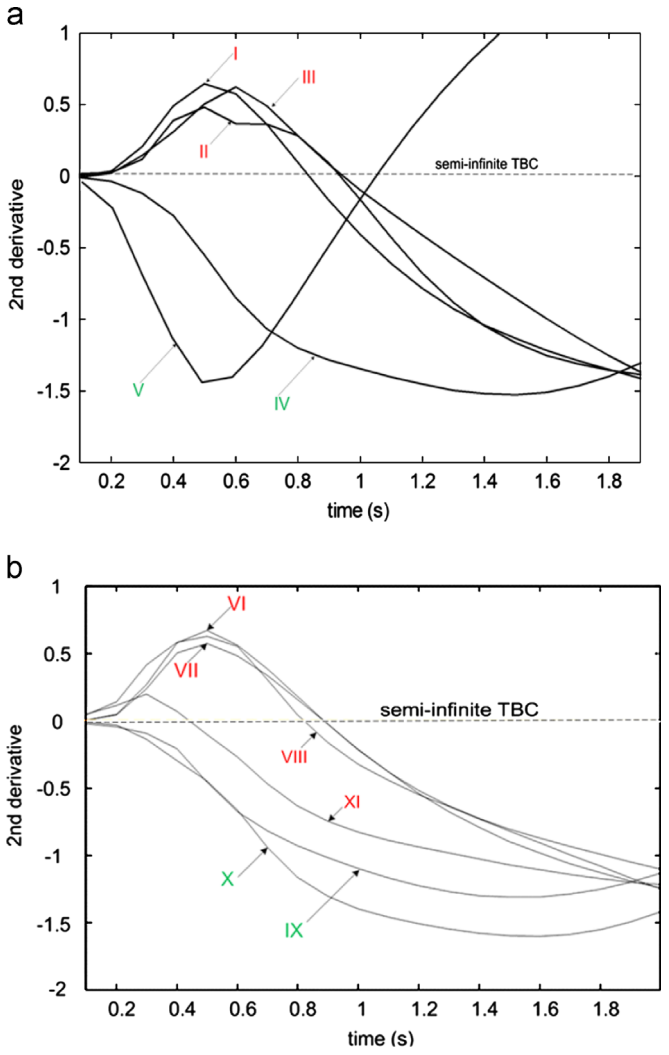

Fig. 16. (a) 2nd Derivative calculated from log–log surface cooling of Fig. 15a; and (b) 2nd derivative calculated from log–log surface cooling of Fig. 15b.

Fig. 15b indicates that the coating above the area XI has been unfortunately partly damaged during the FBH manufacturing process which can be seen in the immediate deviation of the cooling curve from the correct −0.5 slope. However, this is valuable information because, based on the analysis of the log–log surface cooling, it is possible to recognise this abnormality and in this way, the failure of the coating can be located.

It is also very easy to see the increase in the surface temperature caused by blackening by comparing for example the areas IV or IX with the original area V (Fig. 15b). This suggests that the very thin applied layers of ink (areas IV, IX Fig. 15) cause improvements to the radiation of thermal energy in comparison to other sound regions represented here by the area V. Additionally, the thin layer

of graphite (Fig. 15b) absorbs and emits even more energy than the layers of ink (area IV, IX Fig. 15). Indeed, the surface temperature for the areas IV, IX and X was consistently higher than for the area V during the whole observation period (Fig. 15).

Fortunately, the blackened areas IV, IX, X and the original area V show the characteristic minima [1] (Fig. 16a). Interestingly however, for the area V the minimum appears earlier than for the areas IV, IX and X and this minimum also rises rapidly to a maximum. Therefore, the differences in the energy absorption and emission caused by even a very thin layer of material on the TBC surface affect the time of the 2nd derivative minimum and the behaviour immediately afterwards (Fig. 16a). An increase of the energy absorbed results in an increase of the time needed to reach the minima and also in an increase of the time needed to turn the minima to maxima [1]. Fortunately however, the characteristic minima are always present for the sound regions.

As the experiment shows, the effects caused by the applied ink layers on the 2nd derivative are negligible for the defective regions (Fig. 16 except damaged area XI) by showing presence of the characteristic maxima having similar amplitudes and time of appearance.

The analysis of the sound areas and the defective areas suggest that the defect enhancement achieved by the 2nd derivative approach is maintained (defect-maximum, sound area-minimum). Therefore, the 2nd derivative approach is indeed beneficial for the inspection of TBC surfaces in service.

4. Conclusions

It has been explained that transient thermography inspection of unpainted TBC causes problems in interpretation of the results due to its translucency and the discolouration which appears in service. The experimental results show that applying a glass filter and using a long wave IR camera can remove the effects caused by translucency and the afterglow of the flash heating system. Computer simulations have shown that non uniform energy absorption caused by non-uniform colour of TBC affects the thermal contrast from defects and it might also generate false indications of defects. The experimental results have confirmed that the colour of the coating is a very important factor affecting the amount of energy absorbed and emitted from an inspected TBC surface. They demonstrated that non-uniformity in the energy absorption and its emission from a TBC surface due to discolouration may lead to incorrect interpretation of the thermal images in which a darkened, sound area of TBC surface provides a thermal response very similar to the thermal response from a disbond and this situation occurs for a significant fraction of the time after the pulse applied. However, it has been shown that the problem of non uniform colour can be eliminated if the 2nd derivative of surface cooling on a log–log scale is applied as a signal processing technique. This technique applied to transient thermography tests in which a glass filter and a long-wave IR camera are used enhances disbond detection in TBC systems and helps to eliminate false indications of defects; therefore, the reliability of transient thermography for this specific application can be significantly improved.

Acknowledgements

This work has been supported by ALSTOM POWER Switzerland and the Engineering and Physical Sciences Research Council via an Engineering Doctorate studentship for G. Ptaszek in the UK Research Centre for NDE (RCNDE).

References

[1] Ptaszek G, Cawley P, Almond D, Pickering S. Artificial disbonds for calibration of transient thermography inspection of thermal barrier coating systems. NDTE Int 2011;45:71–8.
[2] Shepard S, Favro L, Thomas L. Thermal wave NDT of ceramic coatings. Proc. SPIE 2473. Thermosense XVII 1995;2473:190–3, http://dx.doi.org/10.1117/12.204854.
[3] Sun J. Development of nondestructive evaluation method for ceramic coatings and membranes. In: Proceedings of annual conference in fossil energy materials. Pittsburgh, USA; May 2009.
[4] Shepard S, Hou Y, Lhota J, Wang D, Ahmed T. Thermographic measurement of thermal barrier coating thickness, Thermosense XXVII, vol. 5782, 167-178, 2005.
[5] Computer simulations software COMSOL. www.comsol.com.
[6] Coating manufacturer POETON. ⟨www.poeton.co.uk⟩.
[7] Ceramicmanufacturer TECHNICAL GLASS COMPANY. ⟨www.technicalglass.co.uk⟩.
[8] Adams S. Advanced physics. Oxford, UK: OUP; 2000.
[9] Abuhamad M, Netzelmann U. Dual-band active thermography on infrared transparent materials. In: Proceedings of the 10th international conference on quantitative infrared thermography. Canada; July 2010.
[10] Ringermacher HI, Howard DR. Synthetic Thermal Time-of-Flight (STTOF) Depth Imaging. Rev Prog Quant Nondestr Eval 2001;20:487–91.
[11] Shepard S. System for generating thermographic images using thermographic signal reconstruction. U.S. patent no. 7,724,925 B2; 2010.
[12] Ringermacher HI. Method and apparatus for nondestructive evaluation of insulative coating. U.S. patent no. 7,409,313; 2005.
[13] Ringermacher HI. Synthetic reference thermal imaging method. U.S. patent no. 6,367,969; 2000.
[14] Sun JG. Optical filters for flash lamps in pulsed thermal imaging. U.S. patent no. 7,538,938 B2; 2009.
[15] Chen X. Progressive damage and failure of thermal barrier coatings. Ph.D. dissertation. USA: Wayne State University; 2001.
[16] Maldagu X. Theory and practice of infrared technology for nondestructive testing. New York: A Willey-Interscience Publication; 2001.
[17] Balageas D. Thickness of diffusivity measurements from front-face flash experiments using the TSR (thermographic signal reconstruction) approach. In: Proceedings of the 10th international conference on quantitative infrared thermography. Canada; July 2010.